Journal of Nuclear Medicine, published on August 4, 2016 as doi:10.2967/jnumed.116.177048

Clinical translation of a dual integrin $\alpha_v\beta_3$ and GRPR targeting PET radiotracer ^{68}Ga-BBN-RGD

Jingjing Zhang[1,2], Gang Niu[2], Lixin Lang[2], Fang Li[1], Xinrong Fan[3], Xuefeng Yan[2], Shaobo Yao[1], Weigang Yan[3], Li Huo[1], Libo Chen[1], Zhiyuan Li[4], Zhaohui Zhu[1], Xiaoyuan Chen[2#]

1. Department of Nuclear Medicine, Peking Union Medical College Hospital, Chinese Academy of Medical Sciences and Peking Union Medical College, Beijing 100730, China

2. Laboratory of Molecular Imaging and Nanomedicine (LOMIN), National Institute of Biomedical Imaging and Bioengineering (NIBIB), National Institutes of Health (NIH), Bethesda, Maryland, 20892, USA

3. Department of Urology, Peking Union Medical College Hospital, Chinese Academy of Medical Sciences and Peking Union Medical College, Beijing 100730, China

4. Department of Pathology, Peking Union Medical College Hospital, Chinese Academy of Medical Sciences and Peking Union Medical College, Beijing 100730, China

Jingjing Zhang, Department of Nuclear Medicine, Peking Union Medical College Hospital, Chinese Academy of Medical Sciences, Beijing 100730, China. E-mail: zhangjingjing@pumch.cn

For correspondence or reprints contact either of the following:

Fang Li, Department of Nuclear Medicine, Peking Union Medical College Hospital, Chinese Academy of Medical Sciences, Beijing 100730, China. E-mail: lifang@pumch.cn

Xiaoyuan Chen, National Institutes of Health, 35A Convent Dr., GD937, Bethesda, MD 20892. E-mail: shawn.chen@nih.gov

Running title: ^{68}Ga-BBN-RGD PET

Word count: 4961

ABSTRACT

This study aims to document the first-in-human application of a ^{68}Ga-labeled heterodimeric peptide BBN-RGD (bombesin-RGD) that targets both integrin $\alpha_v\beta_3$ and gastrin releasing peptide receptor (GRPR). We evaluated the safety and assessed the clinical diagnosis value of ^{68}Ga- BBN-RGD positron emission tomography (PET)/x-ray computed tomography (CT) in prostate cancer patients in comparison with ^{68}Ga-BBN. **Methods:** Five healthy volunteers (M 4, F 1, 28–53 y) were enrolled to validate the safety of ^{68}Ga-BBN-RGD. Dosimetry was calculated using the OLINDA/EXM software. A total of 13 patients with prostate cancer (4 newly diagnosed and 9 post-therapy) were enrolled. All the patients underwent PET/CT scans 15–30 min after intravenous injection of 1.85 MBq (0.05 mCi) per kilogram body weight of ^{68}Ga-BBN-RGD, and also accepted ^{68}Ga-BBN PET/CT within 2 weeks for comparison. **Results:** With a mean injected dose of 107.3 ± 14.8 MBq per patient, no side effect was found during the whole procedure and 2 weeks follow-up, demonstrating the safety of ^{68}Ga-BBN-RGD. A patient would be exposed to a radiation dose of 2.90 mSv with an injected dose of 129.5 MBq (3.5 mCi), which is much lower than the dose limit set by the Food and Drug Administration. In 13 patients with prostate cancer diagnosed by biopsy, ^{68}Ga-BBN-RGD PET/CT detected 3 out of 4 primary tumors, 14 metastatic lymph nodes and 20 bone lesions with maximum standardized uptake values (SUV_{max}) of 4.46 ± 0.50, 6.26 ± 2.95, and 4.84 ± 1.57, respectively. Only 2/4 primary tumors, 5 lymph nodes and 12 bone lesions were positive on ^{68}Ga-BBN PET/CT with the SUV_{max} of 2.98 ± 1.24, 4.17 ± 1.89, and 3.61 ± 1.85, respectively. **Conclusion:** This study indicates the safety and the efficiency of a new type of dual integrin $\alpha_v\beta_3$ and GRPR targeting PET radiotracer in prostate cancer diagnosis and staging.

Keywords: BBN-RGD; PET; first-in-human; integrin $\alpha_v\beta_3$; GRPR; prostate cancer

INTRODUCTION

Prostate cancer is the second most frequently diagnosed cancer in men and the fifth leading cause of death worldwide (*1*). Accurate diagnosis and staging of prostate cancer is of topmost importance for effective therapy, especially at early stage (*2*). Currently, the only definitive way to confirm prostate cancer is through prostate biopsy (*3*). However, prostate biopsy is usually deemed necessary by considering several factors including family history, race, abnormal lumps within the prostate, and an elevated serum prostate-specific antigen level. Magnetic resonance imaging (MRI) is one of the major modalities for image-guided diagnosis, but a certain portion of prostate cancer lesions might still be missed using MRI (*4*). In these patients, PET imaging with probes targeting to various prostate cancer specific markers will provide additional molecular information to facilitate lesion detection and staging (*2*).

GRPR is a one important biomarker used for prostate cancer diagnosis (*5*). Various GRPR targeted imaging probes have been developed for non-invasive imaging of GRPR expression (*6-8*). Bombesin (BBN), an amphibian homolog of mammalian gastrin-releasing peptide (GRP), has been extensively used for imaging GRPR, after being labeled with various radionuclides (*6,7,9-12*). Several bombesin related tracers have also been translated into clinic for early phase studies (*13-17*). Previously, we have applied GRPR specific PET tracer ^{68}Ga-NOTA-Aca-BBN(7-14) (denoted as ^{68}Ga-BBN) for first-in-human studies in both healthy volunteers and in patients with both low and high grade gliomas (*18*).

It has been found that both GRPR and integrin $\alpha_v\beta_3$ are overexpressed in neoplastic cells of human prostate cancer (*19*). To target both receptors, a heterodimeric peptide BBN-RGD was synthesized from bombesin(7–14) and c(RGDyK) through a glutamate linker and then labeled with ^{18}F (*20*). Within this heterodimer, the RGD moiety binds to integrin $\alpha_v\beta_3$ receptor, which plays an important role in the regulation of tumor growth, angiogenesis, local invasiveness, and metastatic

potential (*21*). In a PC3 xenograft model, ^{18}F-FB-BBN-RGD had significantly higher tumor uptake compared with monomeric RGD and monomeric BBN peptide tracer analogs at all-time points examined (*20*). A series of preclinical studies using the same strategy have confirmed several advantages of heterodimers including increased number of effective receptors, improved binding affinity and pharmacokinetics (*20,22-24*).

In this study, for the first time, we translated BBN-RGD heterodimer into clinic for the first-in-human study. The safety and dosimetry of ^{68}Ga-BBN-RGD was evaluated in healthy volunteers. The preliminary diagnostic value of ^{68}Ga-BBN-RGD PET/CT was also assessed in patients with primary and/or metastasis prostate cancer.

MATERIALS AND METHODS

Radiopharmaceutical Preparation

The macrocyclic chelator, 1,4,7-triazacyclononane-N,N',N"-triacetic acid (NOTA) conjugated BBN-RGD was synthesized according to a method described in our previous publication (*22*). ^{68}Ga was eluted from a ^{68}Ge/^{68}Ga generator (ITG, Berlin, Germany) using 0.05 M HCl and mixed with 1.25 M NaOAc buffer to adjust pH to 4.0. Radiolabeling of BBN-RGD was performed in a sterile hot cell. The radiochemical purity of the product ^{68}Ga-BBN-RGD exceeded 97%. ^{68}Ga-BBN was synthesized following the procedure reported previously (*18*).

Subject Enrollment

This clinical study was approved by the Institute Review Board of Peking Union Medical College Hospital, Chinese Academy of Medical Sciences and Peking Union Medical College. All subjects signed a written informed consent. Five healthy volunteers (4 M, 1 F; mean age ± standard deviation, 45.2 ± 9.9, age range, 28-53 y; mean weight ± standard deviation, 66.6 ± 8.3 kg, weight range, 55-74 kg) were included in the study. Exclusion criteria consisted of conditions of mental illness, severe liver or kidney disease with serum creatinine > 3.0 mg/dl (270 μM) or any hepatic enzyme level 5 times or more than normal upper limit. Participants were also excluded if they were known to have severe allergy or hypersensitivity to IV radiographic contrast, claustrophobia to accept the PET/CT scanning, or female patients in pregnancy or breast feeding.

A total of 13 patients with prostate cancer (age range, 49-70 y, mean age, 62.4 ± 6.0 y), in which 4 patients were newly diagnosed as prostate cancer by sextant core needle biopsy and not received any prior therapy, and 9 patients underwent prostatectomy or brachytherapy, were enrolled with written informed consent. The inclusion criteria were age 40-80 years, with prostate

neoplasm identified by ultrasound or MRI, needle biopsy diagnosed as prostate cancer, have undergone whole body bone scan, able to provide basic information and sign the written informed consent. The exclusion criteria included claustrophobia, kidney or liver failure, and inability to fulfill the study. The demographics of the patients are listed in Table 1.

The ^{68}Ga-BBN-RGD PET/CT, ^{68}Ga-BBN PET/CT, MRI and MDP bone scan were performed within 2 weeks for comparison. All the 4 newly diagnosed prostate cancer patients underwent radical prostatectomy surgery within one week after ^{68}Ga-BBN-RGD PET/CT. The existence of malignancy in the prostate gland and lymph nodes was confirmed by histological examination with post-operation sampling and/or biopsy. The pathology was determined by two pathologists independently, and reached consensus by referring a third pathologist when there was any discrepancy.

Examination Procedures

For healthy volunteers, the blood pressure, pulse, respiratory frequency, temperature and temperature were measured, and routine blood and urine tests, liver function, renal function were examined immediately before and 24 h after the scan. In addition, any possible side effects during ^{68}Ga-BBN-RGD PET/CT scan and within 1 week after the examination were collected and analyzed as safety data.

No specific subject preparation was requested on the day of ^{68}Ga-BBN-RGD PET/CT scanning. For the volunteers, after the whole-body low-dose CT scan, nearly 111~ 148 MBq (3~4 mCi) of ^{68}Ga-BBN-RGD was injected intravenously, followed by serial whole-body dynamic PET acquisitions. The whole body (from the top of skull to the middle of femur) of each volunteer was covered by 6 bed positions. The acquisition duration was 20 sec/bed position at 1 min post-

injection, 40 sec/bed position at 5 min, 10 min and 15 min post-injection, 2 min/bed position at 30 min, 45 min and 60 min post-injection.

For the patients, ^{68}Ga-BBN-RGD PET/CT Scanning was performed at 15~30 min after tracer administration. For each patient, 1.85 MBq (0.05 mCi) of ^{68}Ga-BBN-RGD per kilogram of body weight was injected intravenously. After a low-dose CT scan, whole body PET acquisition was performed with 2 min per bed position (five to six bed positions depending on the height of the patient). The emission data were corrected for randoms, dead time, scattering, and attenuation. The conventional reconstruction algorithm was used and the images were zoomed with a factor of 1.2. The images were transferred to a MMWP workstation (Siemens) for analysis.

In all patients, a second scan using ^{68}Ga-BBN was performed within 2 weeks for comparison. For each patient, 1.85 MBq (0.05 mCi) of ^{68}Ga-BBN per kilogram of body weight was injected intravenously. The imaging procedure and data analysis is same as that of ^{68}Ga-BBN-RGD PET/CT. MRI was performed with a standard clinical procedure.

Image and Data Analysis

A Siemens MMWP workstation was used for post-processing. Visual analysis was used to determine the general biodistribution and the temporal and inter-subject stability. The volume of interest of normal organs/tissues and concerned lesions were drawn on the serial images. The radioactivity concentration and SUV in the volumes of interest were obtained through the software.

For the volunteers, the dosimetry calculation was performed according to the EANM Dosimetry Guidance (*25*) and calculated using OLINDA/EXM (version 1.1, Vanderbilt University, USA) with the procedure reported in a previous study (*18*). The void time of bladder was set as 60

min. The absorbed doses were calculated by entering the time-integrated activity coefficient for all source organs into OLINDA/EXM for either 73.7 kg adult male or 56.9 kg adult female.

For the patients, regions of interest were drawn manually on the site of lesions using 3D ellipsoid isocontour on each image with the assistance of the corresponding CT images by two experienced nuclear medical physicians. The results were expressed as SUV_{mean} and SUV_{max}.

^{99m}Tc-MDP Bone Scan

For the patients, bone scan images were obtained using a dual-head Siemens single photon emission computed tomography SPECT scanner. Planar images of the whole body skeleton were acquired in the anterior and posterior views 3 h after intravenous injection of 925 MBq (25 mCi) of ^{99m}Tc-MDP.

Immunohistochemical Staining

Representative tumor and lymph node samples were fixed with 10% neutral buffered formalin and embedded in paraffin. After blocking and washing, five μm-thick tissue sections were incubated with mouse anti-human monoclonal antibody against human GRPR (PA5-256791, Thermo Fisher Scientific, Rockford, IL) and integrin $\alpha_v\beta_3$ (1:200, sc-7312, Santa Cruz Biotechnology) respectively. Six fields were randomly selected from each section and observed using a light microscope (BX41, Olympus). For semi-quantification of GRPR and integrin $\alpha_v\beta_3$ expression, five entire high-power fields (×40) containing clusters of malignant cells were identified randomly per slide and scored for intensity and percentage of GRPR and integrin $\alpha_v\beta_3$ staining expression. The procedure was repeated by two independent experienced examiners.

RESULTS

Safety

No adverse events or serious adverse events occurred following ^{68}Ga-BBN-RGD injection for all the healthy volunteers and the patients, and no obvious changes in vital signs or clinical laboratory tests were found before and after the injection of ^{68}Ga-BBN-RGD. For the patients, 1.85 MBq (0.05 mCi) of ^{68}Ga-BBN-RGD per kilogram of body weight was injected intravenously. The median and maximum injected dose was 123.7 ± 11.5 MBq and 146.2 MBq, respectively. The median and maximum injected mass was 12.3 ± 2.6 μg and 15 μg respectively.

Biodistribution and Dosimetry

After intravenous administration, ^{68}Ga-BBN-RGD showed rapid clearance through kidneys with 49.9 ± 10.2% of total injected radioactivity observed in the urine at 30 min p.i. (post injection). Pancreas also had high accumulation with a SUV_{mean} of 10.96 ± 1.10 at 30 min p.i., which is in the line with the known high level expression of GRPR in the pancreas (*26*). Besides, the liver and spleen showed moderate uptake with SUV_{mean} of 1.54 ± 0.24 and 1.80 ± 0.46, respectively. Low background activities in the brain, lung and muscle were found with SUVs of 0.16 ± 0.05, 0.44 ± 0.11 and 0.40 ± 0.16, respectively (Supplemental Table 1, Fig. 1).

The estimated absorbed dose of ^{68}Ga-BBN-RGD for each organ derived from PET/CT images of healthy volunteers is shown in Table 2. Due to the high accumulation of radioactivity in the urinary bladder, the urinary bladder wall had the highest absorbed dose of 0.33 ± 0.16 mSv/MBq, which was followed by the kidneys (0.0647 ± 0.0436 mSv/MBq), and pancreas (0.0523 ± 0.0173 mSv/MBq). The total effective dose equivalent and effective dose were 0.0321 ± 0.0138 and 0.0223 ± 0.0093 mSv/MBq, respectively.

Detection of Primary Prostate Cancer

For the 4 patients with primary prostate cancer, ^{68}Ga-BBN-RGD PET/CT showed positive findings in 3 lesions (75%). The primary lesions were diagnosed by MRI and the diagnosis was confirmed by needle biopsy. The SUV_{mean} and SUV_{max} were 3.26 ± 0.52 and 4.46 ± 0.50, respectively. Two of the 4 lesions were positive on ^{68}Ga-BBN PET/CT with the average mean and maximum SUVs of 2.09 and 2.98, respectively (Fig. 2). In order to further elucidate the findings from PET, we performed immunohistochemical staining against GRPR and integrin $\alpha_v\beta_3$ with the biopsy samples. As shown in Figure 3, both GRPR and integrin positive staining was found in 2 patients, GRPR negative and integrin $\alpha_v\beta_3$ positive staining in one patient, and both GRPR and $\alpha_v\beta_3$ negative stainings in one patient.

Detection of Lymph Node and Bone Metastasis

For all the 13 patients with prostate cancer, ^{68}Ga-BBN-RGD PET/CT detected 14 metastatic lymph nodes and 20 bone lesions. The average and maximum SUVs of all the lymph node metastasis lesions were 3.77 ± 1.65 and 6.26 ± 2.95 at 30 min p.i., respectively. The average and maximum SUVs of all the bone lesions were 3.01 ± 0.84 and 4.84 ± 1.57 at 30 min p.i., respectively. Only 5 lymph node metastases and 12 bone lesions were detected by ^{68}Ga-BBN PET/CT with significantly lower average and maximum SUVs (2.79 ± 1.19 and 4.17 ± 1.89 for lymph nodes and 2.26 ± 1.15 and 3.61 ± 1.85 for bone lesions at 30 min p.i., $P < 0.05$) (Fig. 3 and 4)

In comparison, MRI detected all the 14 lymph nodes in the pelvic cavity. However, only 5 bone lesions located in ilium, pubis, rib, thoracic and lumbar vertebrae were detected by MRI. 11 out of 20 lesions identified by ^{68}Ga-BBN-RGD PET/CT showed positive signal with MDP bone scan. Besides these 20 lesions, 14 abnormal hotspots were shown on MDP SPECT bone scan.

These hotspots were confirmed as benign lesions by MRI and history such as traumatic fracture, vertebral degeneration, and spinal stenosis (Fig. 5).

DISCUSSION

^{68}Ga-BBN-RGD was found to be safe and well tolerated in all healthy volunteers and recruited patients, with no adverse events occurred following tracer injection. With a typical 130 MBq (3.5 mCi) injected activity of ^{68}Ga-BBN, the whole body effective dose is 2.90 mSv, which is much lower than the dose limit set by the by the Food and Drug Administration (*27*). All these data confirmed the safety of ^{68}Ga-BBN for further clinical applications.

One major advantage of heterodimer over the corresponding monomers is the multi-valency effect, resulting in improved binding affinity and increased number of effective receptors (*20,22-24*). Consistently, both ^{68}Ga-BBN-RGD and ^{68}Ga-BBN showed uptake in the primary prostate tumors that are either GPRR (+) or integrin $\alpha_v\beta_3$ (+). However, ^{68}Ga-BBN failed to visualize the lesions that are GPRR (-) and integrin $\alpha_v\beta_3$ (+) while ^{68}Ga-BBN-RGD showed positive result in these cases. It is also reasonable that both tracers had negative results in the lesion with neither GRPR nor integrin $\alpha_v\beta_3$ overexpression, implying that ^{68}Ga-BBN-RGD PET/CT is specific for GRPR and integrin $\alpha_v\beta_3$. Due to limited size of the patient population, the frequency of prostate cancer tumors with both GRPR and integrin $\alpha_v\beta_3$ negative cannot be determined in this study and will need further investigation. With a receptor binding assay in specimens of primary prostate cancer, 37% of samples showed negative bombesin binding (*28*). Thus, it is foreseeable that ^{68}Ga-BBN-RGD PET will increase the detection rate of primary prostate cancer.

About 40 to 60% of men with prostate cancer have lymph node involvement or extra capsular disease at the time of presentation and 70% develop lymph node metastasis during the course (*29*). Although treatable at the early stage, prostate cancer is prone to metastasis, an effective and specific imaging method of detecting both primary and metastatic lesions is thus of critical importance to manage patients with prostate cancer. In 3 patients with LN metastasis, ^{68}Ga-BBN-RGD PET/CT can identify all 14 metastasized LNs as MRI did, which is dramatically better than ^{68}Ga-BBN PET/CT. In addition, the average SUV of ^{68}Ga-BBN-RGD PET/CT is significantly higher than that of ^{68}Ga-BBN PET/CT. Durkan *et al.* (*30*) proposed that prostate cancer cells differentially express specific receptors depending upon factors such as chronicity and metastatic nature. Thus, compounds capable of targeting more than one biomarker would have the ability of binding to both early and metastatic stages of prostate cancer, creating the possibility for more prompt and accurate diagnostic profile for both the primary and metastatic tumors. This may partially explain our results that ^{68}Ga-BBN-RGD PET/CT is better than ^{68}Ga-BBN PET/CT in detecting metastasized LNs.

Autopsy studies suggest that approximately 80-90% of prostate cancer patients have bone metastasis at death although only 6% of men with prostate cancer have metastatic disease at diagnosis (*31*). Skeletal metastasis of prostate cancer is routinely assessed by ^{99m}Tc-MDP bone scan for the staging of prostate cancer. ^{99m}Tc-MDP bone scan is sensitive but lacks specificity since localized skeletal accumulation of ^{99m}Tc-MDP can be observed in the case of trauma and infection. Thus, ^{99m}Tc-MDP bone scan may not be recommended in asymptomatic patients if the serum prostate-specific antigen level is <20 ng/ml in the presence of well-differentiated or moderately differentiated tumors (*3*). In this study, ^{68}Ga-BBN-RGD PET/CT detected 20 bone lesions in 7 patients either with primary prostate cancer or after radical prostatectomy. 11 of these

20 lesions showed positive signal on ^{99m}Tc-MDP bone scan and only 5 of these lesions are detectable with MRI. More importantly, the patients with bone metastases do not necessarily have elevated prostate-specific antigen level (Table 1).

Bisanz *et al.* (*32*) have illustrated a positive role of αv integrins on prostate tumor survival in the bone. Integrin $\alpha_v\beta_3$ activation on tumor cells is essential for the recognition of key bone-specific matrix proteins, suggesting that the $\alpha_v\beta_3$ integrin modulates prostate cancer growth in distant metastasis (*33*). In a recently published clinical study in prostate cancer patients using ^{18}F-Galacto-RGD PET, 58/74 bone-lesions were identified with a detection rate of 78.4% (*34*). Thus RGD moiety in ^{68}Ga-BBN-RGD may play a major role in bone metastasis detection. However, one limitation of this study is the lack of histologic confirmation of the detected bone metastasis. Thus, the GRPR and integrin $\alpha_v\beta_3$ expression status in these metastases are unknown. In addition, the accurate diagnosis and prognosis value of ^{68}Ga-BBN-RGD warrants further larger scale clinical investigations.

Besides BBN based imaging probes, various PET tracers have been used for the detection of prostate cancer such as ^{18}F-FDG, ^{11}C-choline or ^{18}F-fluorcholine, ^{11}C-acetate, ^{18}F-FACBC and prostate-specific membrane antigen (PSMA) targeting agents (*35*). Each of these tracers has advantages and limitations due to the heterogeneity of the disease. We expect that ^{68}Ga-BBN-RGD to play an additive role in staging and detecting prostate cancer, and provide guidance for internal radiation therapy using the same peptide labeled with therapeutic radionuclides.

Conclusion

This study indicates the safety and the efficacy ^{68}Ga-BBN-RGD, a heterodimeric PET tracer targeting both GRPR and integrin $\alpha_v\beta_3$. ^{68}Ga-BBN-RGD PET/CT would have great value in

discerning both primary prostate cancers and metastases in lymph nodes and skeleton, providing tumor staging information and monitoring response of bone metastases to therapy.

Acknowledgment

This work was supported by the Intramural Research Program (IRP) of the National Institute of Biomedical Imaging and Bioengineering (NIBIB), National Institutes of Health (NIH), the National Natural Science Foundation of China projects (81171369, 81171370, and 81271614), and a Special Scientific Research Fund for Public Welfare of Healthcare in China (201402001).

REFERENCES

1. Torre LA, Bray F, Siegel RL, Ferlay J, Lortet-Tieulent J, Jemal A. Global cancer statistics, 2012. *CA Cancer J Clin.* 2015;65:87-108.

2. Maurer T, Eiber M, Schwaiger M, Gschwend JE. Current use of PSMA-PET in prostate cancer management. *Nat Rev Urol.* 2016;13:226-235.

3. Heidenreich A, Bastian PJ, Bellmunt J, *et al.* EAU guidelines on prostate cancer. Part 1: screening, diagnosis, and local treatment with curative intent—update 2013. *Eur Urol.* 2014;65:124-137.

4. Barentsz JO, Richenberg J, Clements R, *et al.* ESUR prostate MR guidelines 2012. *Eur Radiol.* 2012;22:746-757.

5. Ananias HJ, van den Heuvel MC, Helfrich W, de Jong IJ. Expression of the gastrin-releasing peptide receptor, the prostate stem cell antigen and the prostate-specific membrane antigen in lymph node and bone metastases of prostate cancer. *Prostate.* 2009;69:1101-1108.

6. Carlucci G, Kuipers A, Ananias H, *et al.* GRPR-selective PET imaging of prostate cancer using [18 F]-lanthionine-bombesin analogs. *Peptides.* 2015;67:45-54.

7. Chen X, Park R, Hou Y, *et al.* microPET and autoradiographic imaging of GRP receptor expression with ^{64}Cu-DOTA-[Lys^{3}]bombesin in human prostate adenocarcinoma xenografts. *J Nucl Med.* 2004;45:1390-1397.

8. Garrison JC, Rold TL, Sieckman GL, *et al. In vivo* evaluation and small-animal PET/CT of a prostate cancer mouse model using ^{64}Cu bombesin analogs: side-by-side comparison of the CB-TE2A and DOTA chelation systems. *J Nucl Med.* 2007;48:1327-1337.

9. Smith CJ, Volkert WA, Hoffman TJ. Radiolabeled peptide conjugates for targeting of the bombesin receptor superfamily subtypes. *Nucl Med Biol.* 2005;32:733-740.

10. Prasanphanich AF, Nanda PK, Rold TL, *et al.* [^{64}Cu-NOTA-8-Aoc-BBN(7-14)NH_2] targeting vector for positron-emission tomography imaging of gastrin-releasing peptide receptor-expressing tissues. *Proc Natl Acad Sci U S A.* 2007;104:12462-12467.

11. Mansi R, Wang X, Forrer F, *et al.* Development of a potent DOTA-conjugated bombesin antagonist for targeting GRPr-positive tumours. *Eur J Nucl Med Mol Imaging.* 2011;38:97-107.

12. Pourghiasian M, Liu Z, Pan J, *et al.* ^{18}F-AmBF 3-MJ9: A novel radiofluorinated bombesin derivative for prostate cancer imaging. *Bioorg Med Chem.* 2015;23:1500-1506.

13. Van de Wiele C, Dumont F, Dierckx RA, *et al.* Biodistribution and dosimetry of ^{99m}Tc-RP527, a gastrin-releasing peptide (GRP) agonist for the visualization of GRP receptor–expressing malignancies. *J Nucl Med.* 2001;42:1722-1727.

14. Van de Wiele C, Phonteyne P, Pauwels P, *et al.* Gastrin-releasing peptide receptor imaging in human breast carcinoma versus immunohistochemistry. *J Nucl Med.* 2008;49:260-264.

15. A Nock B, Maina T. Tetraamine-coupled peptides and resulting ^{99m}Tc-radioligands: An effective route for receptor-targeted diagnostic imaging of human tumors. *Curr Top Med Chem.* 2012;12:2655-2667.

16. Ananias HJ, Yu Z, Dierckx RA, *et al.* 99mtechnetium-HYNIC (tricine/TPPTS)-Aca-bombesin (7–14) as a targeted imaging agent with microSPECT in a PC-3 prostate cancer xenograft model. *Mol Pharm.* 2011;8:1165-1173.

17. Ananias HJ, Yu Z, Hoving HD, *et al.* Application of 99mTechnetium-HYNIC (tricine/TPPTS)-aca-bombesin (7-14) SPECT/CT in prostate cancer patients: a first-in-man study. *Nucl Med Biol.* 2013;40:933-938.

18. Zhang J, Li D, Lang L, *et al.* ^{68}Ga-NOTA-Aca-BBN(7-14) PET/CT in healthy volunteers and glioma patients. *J Nucl Med.* 2016;57:9-14.

19. Beer M, Montani M, Gerhardt J, *et al.* Profiling gastrin-releasing peptide receptor in prostate tissues: Clinical implications and molecular correlates. *Prostate.* 2012;72:318-325.

20. Li Z-B, Wu Z, Chen K, Ryu EK, Chen X. ^{18}F-labeled BBN-RGD heterodimer for prostate cancer imaging. *J Nucl Med.* 2008;49:453-461.

21. Niu G, Chen X. Why integrin as a primary target for imaging and therapy. *Theranostics.* 2011;1:30-47.

22. Liu Z, Niu G, Wang F, Chen X. ^{68}Ga-labeled NOTA-RGD-BBN peptide for dual integrin and GRPR-targeted tumor imaging. *Eur J Nucl Med Mol Imaging.* 2009;36:1483-1494.

23. Liu Z, Yan Y, Liu S, Wang F, Chen X. ^{18}F, ^{64}Cu, and ^{68}Ga labeled RGD-bombesin heterodimeric peptides for PET imaging of breast cancer. *Bioconjugate Chem.* 2009;20:1016-1025.

24. Eder M, Schafer M, Bauder-Wust U, Haberkorn U, Eisenhut M, Kopka K. Preclinical evaluation of a bispecific low-molecular heterodimer targeting both PSMA and GRPR for improved PET imaging and therapy of prostate cancer. *Prostate.* 2014;74:659-668.

25. Lassmann M, Chiesa C, Flux G, Bardies M. EANM Dosimetry Committee guidance document: good practice of clinical dosimetry reporting. *Eur J Nucl Med Mol Imaging.* 2011;38:192-200.

26. Gonzalez N, Moody TW, Igarashi H, Ito T, Jensen RT. Bombesin-related peptides and their receptors: recent advances in their role in physiology and disease states. *Curr Opin Endocrinol Diabetes Obes.* 2008;15:58-64.

27. Mittra ES, Goris ML, Iagaru AH, *et al.* Pilot pharmacokinetic and dosimetric studies of (18)F-FPPRGD2: a PET radiopharmaceutical agent for imaging αvβ3 integrin levels. *Radiology.* 2011;260:182-191.

28. Sun B, Halmos G, Schally AV, Wang X, Martinez M. Presence of receptors for bombesin/gastrin-releasing peptide and mRNA for three receptor subtypes in human prostate cancers. *The prostate.* 2000;42:295-303.

29. Vag T, Heck MM, Beer AJ, *et al.* Preoperative lymph node staging in patients with primary prostate cancer: comparison and correlation of quantitative imaging parameters in diffusion-weighted imaging and ^{11}C-choline PET/CT. *E Eur Radiol.* 2014;24:1821-1826.

30. Durkan K, Jiang Z, Rold TL, *et al.* A heterodimeric [RGD-Glu-[^{64}Cu-NO2A]-6-Ahx-RM2] alphavbeta3/GRPr-targeting antagonist radiotracer for PET imaging of prostate tumors. *Nucl Med Biol.* 2014;41:133-139.

31. Bubendorf L, Schöpfer A, Wagner U, *et al.* Metastatic patterns of prostate cancer: an autopsy study of 1,589 patients. *Hum Pathol.* 2000;31:578-583.

32. Bisanz K, Yu J, Edlund M, *et al.* Targeting ECM–integrin interaction with liposome-encapsulated small interfering RNAs inhibits the growth of human prostate cancer in a bone xenograft imaging model. *Mol Ther.* 2005;12:634-643.

33. McCabe N, De S, Vasanji A, Brainard J, Byzova T. Prostate cancer specific integrin αvβ3 modulates bone metastatic growth and tissue remodeling. *Oncogene.* 2007;26:6238-6243.

34. Beer AJ, Schwarzenbock SM, Zantl N, *et al*. Non-invasive assessment of inter-and intrapatient variability of integrin expression in metastasized prostate cancer by PET. *Oncotarget.* 2016;7:28151-28159.

35. Kitajima K, Yamamoto S, Fukushima K, Minamimoto R, Kamai T, Jadvar H. Update on advances in molecular PET in urological oncology. *Jpn J Radiol.* 2016;34:470-485.

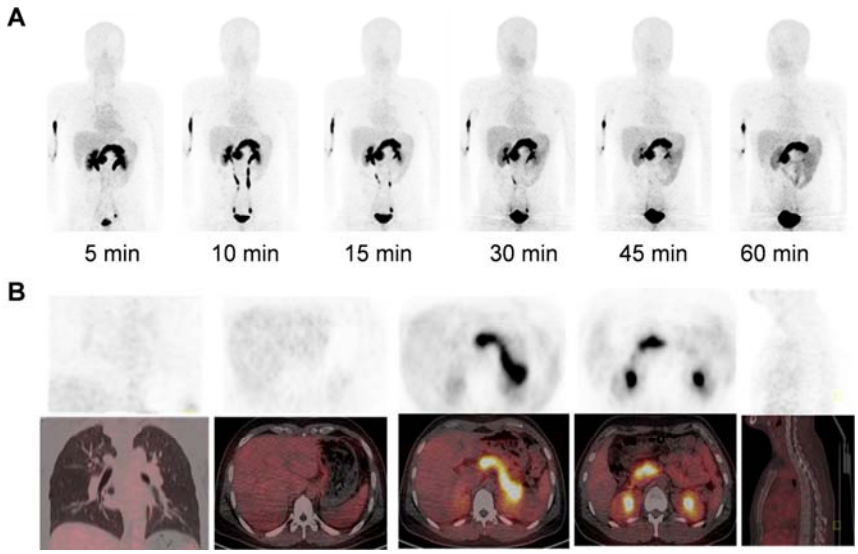

FIGURE 1. (A) Multiple-time-point whole-body maximum-intensity-projection (MIP) PET images at 1, 5, 10, 15, 30, 45, 60 min after intravenous administration of ^{68}Ga-BBN-RGD in a 47-year-old male volunteer. (B) PET/CT showed tracer uptake in major organs at 30 min after intravenous administration of 129.5 MBq (3.5 mCi) of ^{68}Ga- BBN-RGD to a male volunteer.

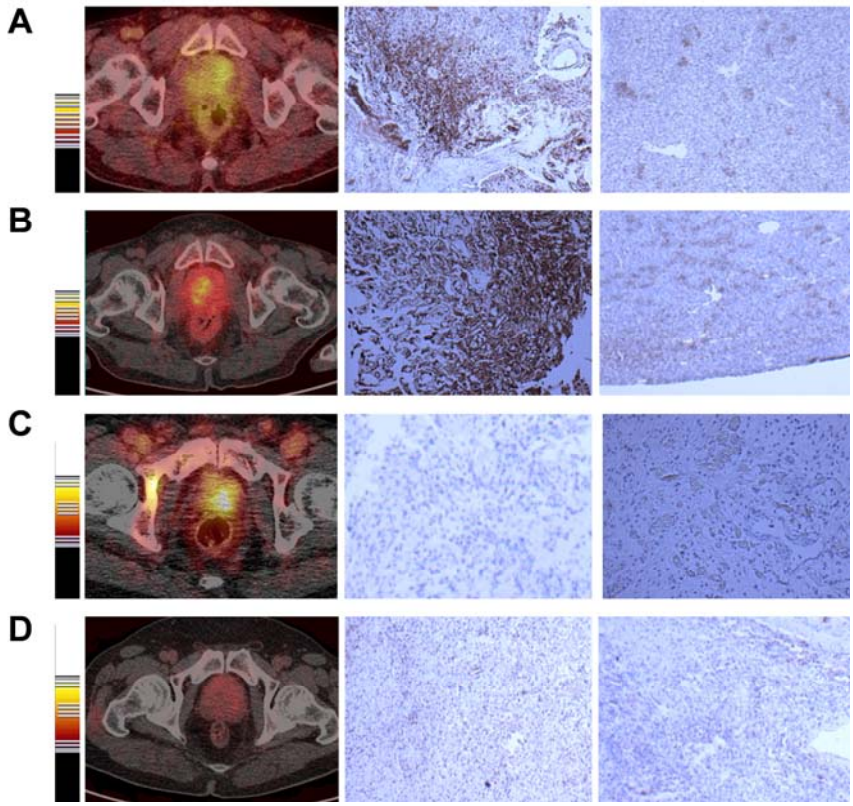

FIGURE 2. ^{68}Ga-BBN-RGD PET/CT of the primary tumors of 4 prostate cancer patients. Immunohistologic staining against GRPR and integrin $\alpha_v\beta_3$ was performed with the biopsy samples. (A&B) GRPR (+) and $\alpha_v\beta_3$ (+), (C) GRPR (-) and $\alpha_v\beta_3$ (+), and (D) GRPR (-) and $\alpha_v\beta_3$ (-).

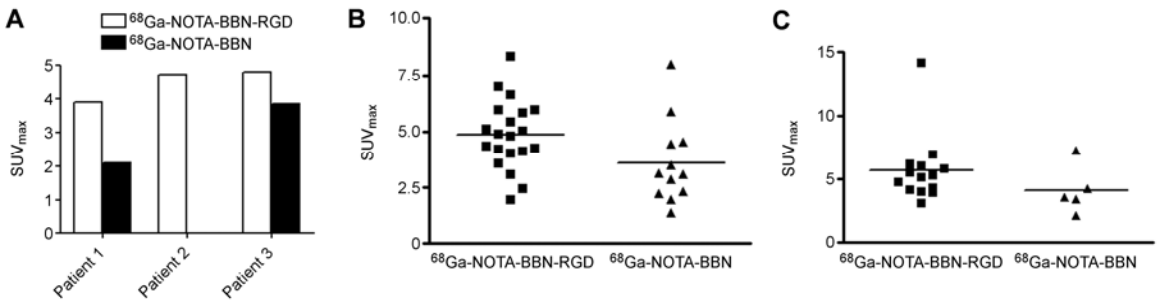

FIGURE 3. Quantitative comparison between ^{68}Ga-BBN-RGD PET/CT and ^{68}Ga-BBN PET/CT in primary tumor (A), bone metastases (B) and lymph node metastases (C).

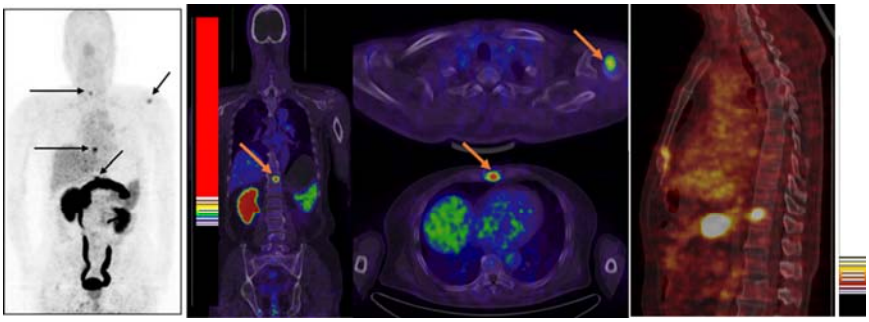

FIGURE 4. ^{68}Ga-BBN PET/CT of a 64-year-old man newly diagnosed as prostate cancer by biopsy. Multiple bone metastasis lesions (arrow) were detected.

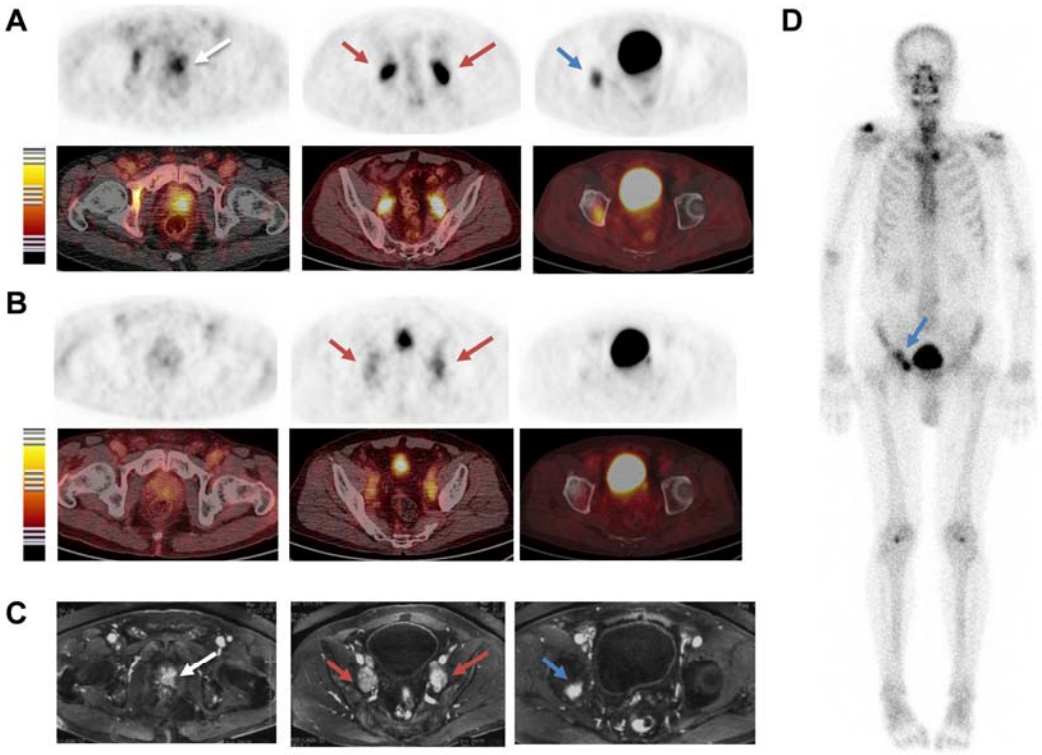

FIGURE 5. Comparison of ^{68}Ga-BBN-RGD PET/CT (A), ^{68}Ga-BBN PET/CT (B), MRI (C) and ^{99m}Tc-MDP bone scan (D) in a 63-year-old man diagnosed as prostate cancer (white arrow) with lymph node involvement (red arrow) and bone metastasis (blue arrow) before prostatectomy. Both ^{68}Ga-BBN-RGD PET/CT and MRI detected the primary tumors, multiple lymph nodes involvement, and bone metastasis lesion, while ^{68}Ga-BBN PET/CT only detected lymph node metastases.

TABLE 1. Patient demographics

No.	Age (yr)	PSA (ng/ml)	GS	Treatment	Bone scan	MRI	^{68}Ga-BBN-RGD PET/CT	^{68}Ga-BBN PET/CT
1	69	109.1	7	RP	(-)	PT	PT	PT
2	61	7.31	7	RP	(-)	PT	PT	PT
3	55	30.3	9	RP	(-)	PT	(-)	(-)
4	68	25.59	7	RP	(+)	PT/ LNs/BM	PT/LNs/BM	LNs
5	64	36.1	7	BT + ADT	(-)	(-)	BM	BM
6	78	108.1	7	RP + RT + C	(+)	BM	BM	(-)
7	67	5.34	6	RT+ADT	(-)	(-)	(-)	(-)
8	62	20.2	8	ADT	(+/-)	BM	BM	BM
9	79	15.79	8	BT + C	(+)	LNs/BM	LNs/ BM	BM
10	59	5.78	8	RP + RT	(+/-)	BM	BM	BM
11	58	4.15	7	RP	(+/-)	(-)	(-)	(-)
12	70	105	7	BT + C	(+)	(-)	BM	(-)
13	65	4.1	9	RP + RT	(-)	LNs	LNs	(-)

RP, radical prostatectomy; RT, radiation therapy; ADT, androgen deprivation therapy; BT, brachytherapy; C, chemotherapy; LNs, Lymph nodes involvement; BM, Bone metastasis; GS, Gleason score; PT, primary tumor; PSA, prostate-specific antigen

TABLE 2. Estimated absorbed dose after intravenous administration of ^{68}Ga-BBN-RGD (mSv/MBq, n = 5, 4 males and 1 female, SD, standard deviation)

Target organ	Mean	SD
Adrenals	4.70E-03	1.45E-03
Brain	1.32E-03	1.80E-04
Breasts	2.50E-03	1.00E-03
Gallbladder Wall	4.88E-03	1.25E-03
LLI Wall	7.16E-03	1.71E-03
Small Intestine	5.02E-03	1.38E-03
Stomach Wall	3.95E-03	1.18E-03
ULI Wall	4.70E-03	1.36E-03
Heart Wall	8.38E-03	2.31E-03
Kidneys	6.47E-02	4.36E-02
Liver	1.55E-02	6.11E-03
Lungs	3.88E-03	8.39E-04
Muscle	4.48E-03	1.09E-03
Ovaries	6.97E-03	1.70E-03
Pancreas	5.23E-02	1.73E-02
Red Marrow	4.89E-03	7.66E-04
Osteogenic Cells	5.32E-03	1.58E-03
Skin	2.64E-03	9.64E-04
Spleen	1.14E-02	4.25E-03
Testes	4.85E-03	1.04E-03
Thymus	2.90E-03	1.01E-03
Thyroid	2.67E-03	9.75E-04
Urinary Bladder Wall	3.33E-01	1.60E-01
Uterus	1.55E-02	
Total Body	5.43E-03	1.56E-03
Effective Dose Equivalent	3.21E-02	1.38E-02
Effective Dose	2.23E-02	9.26E-03